

Received:  
02 April 2021Revised:  
09 June 2021Accepted:  
21 June 2021

© 2021 The Authors. Published by the British Institute of Radiology under the terms of the Creative Commons Attribution-NonCommercial 4.0 Unported License <http://creativecommons.org/licenses/by-nc/4.0/>, which permits unrestricted non-commercial reuse, provided the original author and source are credited.

Cite this article as:

Pötter-Lang S, Ba-Ssalamah A, Bastati N, Messner A, Kristic A, Ambros R, et al. Modern imaging of cholangitis. *Br J Radiol* 2021; **94**: 20210417.

## REVIEW ARTICLE

# Modern imaging of cholangitis

<sup>1</sup>SARAH PÖTTER-LANG, <sup>1</sup>AHMED BA-SSALAMAH, <sup>1</sup>NINA BASTATI, <sup>1</sup>ALINA MESSNER, <sup>1</sup>ANTONIA KRISTIC, <sup>1</sup>RAPHAEL AMBROS, <sup>1</sup>ALEXANDER HEROLD, <sup>1</sup>JACQUELINE C. HODGE and <sup>2</sup>MICHAEL TRAUNER

<sup>1</sup>Department of Biomedical Imaging and Image-guided Therapy, Medical University of Vienna, Vienna, Austria

<sup>2</sup>Division of Gastroenterology and Hepatology, Department of Internal Medicine III, Medical University of Vienna, Vienna, Austria

Address correspondence to: Mr Ahmed Ba-Ssalamah  
E-mail: [ahmed.ba-ssalamah@meduniwien.ac.at](mailto:ahmed.ba-ssalamah@meduniwien.ac.at)

### ABSTRACT

Cholangitis refers to inflammation of the bile ducts with or without accompanying infection. When intermittent or persistent inflammation lasts 6 months or more, the condition is classified as chronic cholangitis. Otherwise, it is considered an acute cholangitis. Cholangitis can also be classified according to the inciting agent, e.g. complete mechanical obstruction, which is the leading cause of acute cholangitis, longstanding partial mechanical blockage, or immune-mediated bile duct damage that results in chronic cholangitis.

The work-up for cholangitis is based upon medical history, clinical presentation, and initial laboratory tests. Whereas ultrasound is the first-line imaging modality used to identify bile duct dilatation in patients with colicky abdominal pain, cross-sectional imaging is preferable when symptoms cannot be primarily localised to the hepatobiliary system. CT is very useful in oncologic, trauma, or postoperative patients. Otherwise, magnetic resonance cholangiopancreatography is the method of choice to diagnose acute and chronic biliary disorders, providing an excellent anatomic overview and, if gadoteric acid is injected, simultaneously delivering morphological and functional information about the hepatobiliary system. If brush cytology, biopsy, assessment of the prepapillary common bile duct, stricture dilatation, or stenting is necessary, then endoscopic ultrasound and/or retrograde cholangiography are performed. Finally, when the pathologic duct is inaccessible from the duodenum or stomach, percutaneous transhepatic cholangiography is an option. The pace of the work-up depends upon the severity of cholestasis on presentation. Whereas sepsis, hypotension, and/or Charcot's triad warrant immediate investigation and management, chronic cholestasis can be electively evaluated. This overview article will cover the common cholangitides, emphasising our clinical experience with the chronic cholestatic liver diseases.

### INTRODUCTION

Cholangitis refers to bile duct inflammation which, untreated, ultimately destroys cholangiocytes, causing scarring and/or ductopenia. Subsequently, the accumulation of bile constituents will damage the hepatocytes, leading to fibrosis, end-stage biliary cirrhosis, and finally, liver failure.<sup>1,2</sup> Cholangitis is classified as acute (AC) vs chronic (CC), according to its aetiology, or site of bile flow impairment.<sup>3,4</sup> CC mandates that symptoms last at least 6 months, otherwise, it is labeled AC.<sup>1</sup>

Cholangitis may affect the intrahepatic ducts (IHD) and extrahepatic ducts (EHD). However, intrahepatic cholestasis can also originate at the hepatocyte level through impaired canalicular bile secretion caused by genetic defects, drugs, or inflammatory processes.<sup>5-7</sup> Like many other chronic liver diseases, primary biliary cholangitis (PBC) and primary sclerosing cholangitis (PSC) may

be characterised by clinically quiescent phases and intermittent bouts of bile duct inflammation or infection, *i.e.* true bacterial “cholangitis”.

Extrahepatic duct (EHD) cholangitis, involving the common hepatic (CHD) or common bile ducts (CBDs), can be intrinsic, e.g. strictures in PSC, cholangiocarcinoma (CCA), and stones, or extrinsic, e.g. lymphadenopathy, masses, or cysts.<sup>8,9</sup> Clinical, serologic, and imaging features help to differentiate the various types of cholangitides.<sup>10</sup>

The typical features of AC, including fever, colicky upper abdominal pain, and tenderness, are most often due to choledocholithiasis.<sup>11</sup> These symptoms may also follow interventions, e.g. biliary-enteric anastomotic stenosis, or indwelling biliary stent malfunction.<sup>12</sup> Non-bacterial, e.g. immune-mediated or viral cholangitides, typically evolve more slowly.<sup>13</sup> As cholangitis differs between

Table 1. Aetiology: acute and chronic cholangitis

Etiology	Acute cholangitis	Chronic cholangitis
Obstruction	Biliary stones	Biliary strictures Anastomotic strictures post-OLT NAS post-OLT Neoplasms (benign or malignant)
Infectious cholangitides	Bacterial ( <i>E.coli</i> , <i>Klebsiella</i> , <i>Enterococcus</i> , <i>Enterobacter</i> )	RPC Parasitic infection Viral (HBV, HCV, HEV, HSV CMV, EBV) AIDS-Cholangiopathy
Immunologic		PSC PBC IgG4 holangitis AIDS cholangiopathy
Toxic	Drugs	DILI Intra-arterial chemotherapy
Ischaemic cholangiopathy		Secondary sclerosing cholangitis
Congenital		Choledochal (Todani), duodenal diverticula

DILI, drug induced liver injury; OLT, orthotopic liver transplantation; PBC, primary biliary cholangitis; PSC, primary sclerosing cholangitis; RPC, recurrent pyogenic cholangitis.

immunocompetent and immunocompromised patients, the host's immune status may be inferred from imaging. Viruses (*e.g.* CMV, HIV), either by direct invasion, immune-mediated cell destruction, or associated bacterial or opportunistic infection, may cause cholangitis, particularly in immunocompromised patients (Table 1).<sup>14</sup>

Laboratory tests help determine the severity and, sometimes, even the aetiology of cholangitis. Elevated serum alkaline phosphatase (ALP) and  $\gamma$ -glutamyl transpeptidase (GGT) are indicative of cholestatic disease, with bilirubin increasing only in the late stages of fibroproliferative cholangiopathies, such as PBC and PSC, or when complicated by dominant/relevant strictures (*e.g.* PSC).<sup>15</sup> Importantly, ALP and GGT may take 24–48 h to increase significantly and may still be normal in acute biliary obstruction, while a hepatitis profile, *i.e.* elevated aspartate alanine aminotransferase (ALT), which reflects hepatocellular damage from accumulating bile acids, may initially dominate. Markers of systemic inflammation, including leukocytosis and elevated C-reactive protein, suggest bacterial cholangitis. Eosinophilia (*e.g.* parasitic infections), various autoimmune antibody titers (*e.g.* antimicrobial antibody (AMA) in PBC), EBV or CMV serology, blood cultures, and tumour markers (*e.g.* CA 19–9) can direct the diagnosis.<sup>16</sup> Caveat: CA 19–9 can rise in non-tumoural biliary obstruction and bacterial cholangitis, and conversely, may remain normal in Lewis-negative “non-secretors” with a tumour.<sup>17,18</sup>

Imaging usually starts with ultrasound<sup>19</sup> since it is very sensitive for gallbladder evaluation. Ultrasound has a sensitivity and specificity exceeding 95% for gallstones.<sup>20</sup> However, ultrasound has 75% sensitivity for choledocholithiasis when the CBD is dilated, 50% when the CBD is normal-caliber and can even be 40% for small stones or stones lodged near the ampulla when obscured by bowel gas.<sup>21</sup> Following recent surgery, trauma, or biliary intervention, CT may be more helpful in excluding mechanical obstruction.<sup>22</sup> In patients with unexplained cholestasis, a negative

ultrasound should be followed by magnetic resonance cholangiopancreatography (MRCP) to detect the presence and site(s) of duct involvement.<sup>23</sup> Contrast enhanced-MRI or MR cholangiography (MRC) with hepatobiliary contrast agents (gadoteric acid, Primovist<sup>®</sup>) provides excellent detection of subtle morphologic changes while evaluating liver function in the chronic cholangitides.<sup>24,25</sup> Endoscopic retrograde cholangiopancreatography (ERCP) or percutaneous transhepatic cholangiography (PTC) are reserved for biliary decompression, while ERCP or endoscopic ultrasound (EUS) aid in tissue diagnosis (Table 2).<sup>26</sup>

#### Acute cholangitis

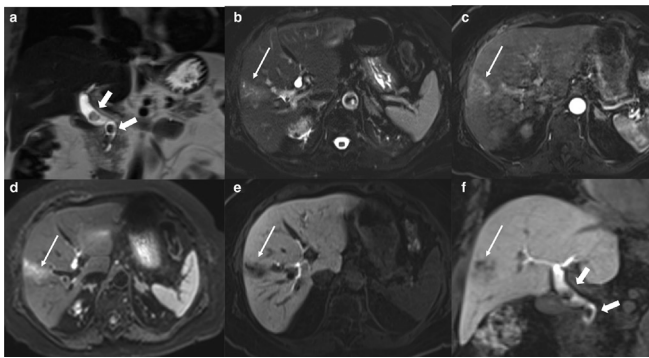
Acute bacterial cholangitis (AC) is the most common biliary tree affliction, mainly caused by calculi in middle-aged obese females.<sup>27</sup> Less often, stricture(s) or extrinsic duct compression, or rarely, bile duct cysts or duodenal diverticula, cause gradual obstruction.<sup>28</sup> Seldom does intraductal pressure exceed 25 mm H<sub>2</sub>O. However, if this threshold is crossed, cholangitis occurs due to bile reflux into veins and lymphatics.<sup>9</sup> According to the Tokyo Guidelines, clinical presentation, laboratories, and imaging are necessary for a diagnosis of AC.<sup>29</sup> Charcot's triad is seen in 70%.<sup>13</sup> However, diagnosing AC in underlying chronic cholestasis is challenging since symptoms may be atypical and criteria are not universal.<sup>30</sup> On MRI, periportal tracking and high-signal-intensity (SI), wedge-shaped segmental cholangitis, due to lymphatic inflammation may be visible even in asymptomatic patients, preceding the increase in cholestatic labs (Figure 1). Furthermore, liver enzymes may remain at baseline even when *E. coli* and other gut bacteria are present, especially if limited to smaller liver segments.<sup>31</sup> Haematogenous spread of bacteria to the liver is a critical pathogenic factor for cholangitic liver abscesses<sup>32</sup> (Figure 2). However, as cholangitis spreads, systemic inflammatory response syndrome (SIRS) turns into sepsis, with or without multiorgan failure, increasing mortality risk to 50%.<sup>33</sup> Urgent imaging to determine the site of the obstruction, should be followed by ERCP or percutaneous biliary drainage within 24 h.<sup>29,34</sup> In patients with AC refractory to treatment,

Table 2. Imaging features and management of most common cholangitides and cholestases

Disease entity	Main imaging features	Other diagnostic tests	Associated conditions	Treatment
Acute Cholangitis Acute Suppurative Cholangitis	CBD stone, bile duct dilatation		Gallstones	ERCP or PTC drainage
	Pus within bulging bile duct(s)			ERCP or PTC drainage
Oriental Cholangitis	IHD stones without gallstones, Segmental liver atrophy	Possible eosinophilia	Clonorchis sinensis or Ascaris lumbricoides	Praziquantel or albendazole/ ivermectin
Fasciola Hepatica	Tunnels and caves R liver lobe	Possible eosinophilia		Triclabendazole
Hepatic Schistosomiasis	Cirrhosis	Possible eosinophilia		Praziquantel
Echinococcus Granulosus	Hydatid cysts	Possible eosinophilia		Albendazole, PAIR (if no biliary tree contact) or surgery
AIDS Cholangiopathy	PSC-like pattern	Low CD4 counts Cryptosporidium, CMV as additional causative factors	HAART-resistance	ERCP
Post-transplant Cholangiopathy	Anastomotic biliary stricture			ERCP
	Multiple NAS, intraductal casts, intrahepatic biloma			ERCP or re- transplantation
Secondary Sclerosing Cholangitis	PSC-like pattern		Iatrogenic (e.g., surgery, TACE) SSC-CIP (SSC- in critically ill patients)	Liver transplant
			Toxins	Discontinue exposure
			Langerhans Cell Histiocytosis	Steroids
			Mastocytosis	Steroids Imatinib, Ilotinib or Dasatinib
PSC	IHD and/or EHD strictures	Elevated ALP, Possible atypical pANCA	IBD	No established medical therapy, UDCA frequently used Liver transplant
PBC	No visible IHD or EHD dilatation on MRI, splenomegaly	Elevated ALP, Positive titers AMA, Positive titers ANA-PBC specific	Hashimoto's Sjogren's Celiac disease	UDCA Second line: obeticholic acid, fibrates
IgG4 Sclerosing Cholangitis	Solitary IHD or EHD stricture	IgG4 levels > 4x normal	Autoimmune pancreatitis Salivary gland and/or retroperitoneal inflammation	Steroids, azathioprine Second line: Rituximab
DILI	PSC-like pattern or PBC-like pattern		Chemotherapy, Drugs, Anabolic steroids	Discontinue drugs/steroids
Stauffer Syndrome	Non-specific		Paraneoplastic syndrome	Treat underlying malignancy
Graft Versus Host Disease	Non-specific		Gastrointestinal symptoms	Steroids, cyclosporine
Intrahepatic Cholestasis of Pregnancy	Not usually imaged beyond ultrasound			UDCA anti-pruritic drugs

ALP, Alkaline phosphatase; CBD, common bile duct; DILI, drug-induced liver injury; EHD, Extrahepatic bile duct; ERCP, endoscopic retrograde cholangiopancreatography; HAART, highly active antiretroviral therapy; HBV, Hepatitis B virus; HCV, Hepatitis C virus; IBD, Inflammatory bowel disease; IHD, Intrahepatic bile duct; NAS, Nonanastomotic strictures; PBC, primary biliary cholangitis; PSC, primary sclerosing cholangitis; PTC, Percutaneous transhepatic cholangiography; TACE, Transcatheter arterial chemoembolisation; UDCA, Ursodeoxycholic acid.

Figure 1. 40-yr-old female with acute segmental cholangitis in the right liver lobe due to CBD calculi. (A) Coronal HASTE shows two, round, low-signal-intensity filling defects (thick arrows) within a distended common bile duct. (B) Axial HASTE image shows a wedge-shaped peripheral area of mildly increased SI (arrow) in segment 6. (C) Axial T1 GRE gadoxetic acid-enhanced, arterial phase, shows a wedge-shaped peripheral hyperenhancing area in segment 6 (arrow) due to inflammation. (D) Axial DWI ( $b$  300 s/mm<sup>2</sup>) confirms the wedge-shaped area of cholangitis (arrow), here clearly definable. (E, F) Axial and coronal T1 GRE gadoxetic acid-enhanced, 20 min after injection, in the HBP shows a non-enhancing parenchymal area corresponding to functional impairment (arrow) and two filling defects (thick arrows) in the CBD due to stones. There is not complete obstruction, as the contrast media excretion is preserved within the HBP. CBD, common bile duct; DWI, diffusion-weighted imaging; HBP, hepatobiliary phase; SI, signal intensity.

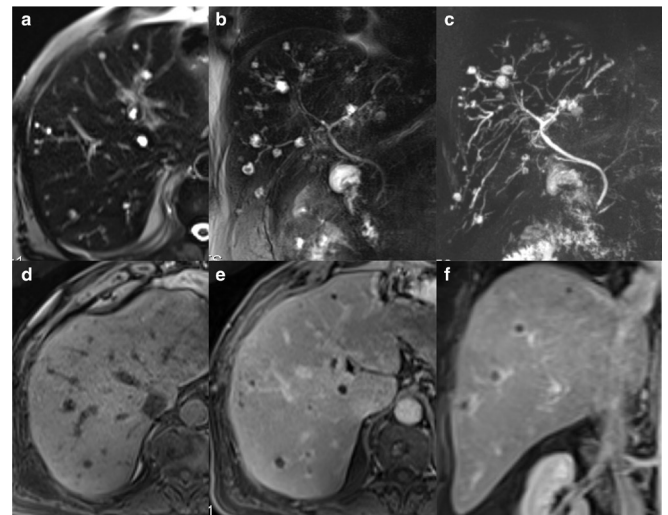


contrast-enhanced CT (CE-CT) or MRI (CE-MRI) should be done to evaluate the liver parenchyma for abscess(es).<sup>35</sup> MRCP is ideal for complete localisation and characterisation of duct pathology.<sup>19,36</sup>

Normal IHDs are small in calibre and only faintly seen on CE-CT or CE-T1-weighted MRI, but can be seen more clearly on T2-weighted imaging and hepatobiliary CE-MRC.<sup>23</sup> Using a hepatobiliary contrast agent, we can visualise the biliary tree and its patency and function (Figure 1). In 85% of acute cholangitis, the CBD appears smooth with symmetric wall thickening, and infrequently, with IHD wall enhancement as well. Liver parenchymal enhancement occurs in the arterial-phase only in approximately 60%, delayed-phase only in nearly 15%, and both phases in one-third. On T2-weighted images, approximately 70% have parenchymal wedge-shaped or periductal high SI<sup>37</sup> (Figure 1). Diffusion-weighted imaging (DWI) is even more sensitive to cholangitis,<sup>38</sup> and can distinguish it from perfusion defects, such as transient hepatic intensity defects (THID).<sup>39</sup> Although both show arterial-phase enhancement, only cholangitis has a DWI correlate (Figure 1). Furthermore, cholangitis appears hypointense on the 20 min hepatobiliary-phase (HBP) of gadoxetic acid-enhanced MRI due to oedema and fibrosis in acute and chronic cholangitis, respectively<sup>40</sup> (Figure 1).

Portal vein thrombosis and/or hepatic abscess(es) are complications in bacterial cholangitis.<sup>41,42</sup> Pus within the bile duct(s) *i.e.* low SI on heavily T2-weighted images and moderate SI on

Figure 2. 60-yr-old male with diverticulitis and right upper quadrant pain. Acute cholangitis with multiple small hepatic abscesses. (A) Axial and (B) coronal HASTE with fat sat show multiple small hyperintense lesions along the bile ducts predominantly in the right liver lobe consistent with abscesses. (C) Coronal MRCP T2-weighted MIP shows the close relationship of these small abscesses to the biliary tree. (D) Axial T1 GRE shows multiple small round hypointense lesions in the right liver lobe. (E) Axial and (F) coronal gadolinium chelate-enhanced T1-weighted GRE with fat sat shows peripheral ring enhancement of these small abscesses. MIP, maximum intensity projection; MRCP, magnetic resonance cholangiopancreatography.



fat-suppressed T1-weighted images, or a bulging, enhancing bile duct papilla that exceeds 1 cm (specificity 86%) is diagnostic of acute suppurative cholangitis, which complicates AC in approximately 60% and warrants immediate drainage.<sup>43</sup>

## Chronic cholangitis

### Infectious

Recurrent pyogenic cholangitis (RPC), previously known as Oriental cholangiohepatitis, is typically seen in patients who reside in or who have immigrated from Southeast Asia. It is characterised by IHD and EHD strictures and dilatation with pigment stone formation, usually due to parasites, *e.g.* *Clonorchis sinensis* or *Ascaris lumbricoides*.<sup>44</sup> Delayed diagnosis leads to chronic bile stasis with subsequent hepatolithiasis, segmental liver atrophy, and cholangiocarcinoma (CCA). The most helpful imaging findings are the presence of large IHD stones in the absence of gallbladder calculi, which occur in 80%, sparing of the EHDs, and high-protein content calculi that appear bright on T1- and dark on T2-weighted sequences.<sup>37</sup> Either due to bowel gas reflux or superinfection with gas-forming bacteria from the gut (*e.g.* *Escherichia coli*), pneumobilia is also common.

Other common hepatobiliary parasites endemic to Asia, Egypt, and Africa and, infrequently, Europe, include Schistosomiasis. Echinococcosis and, *Fasciola hepaticus* are universal. On imaging, parasites cause filling defects within the bile ducts, and sometimes blockage of the ducts leading to upstream dilatation.<sup>37</sup>

Figure 3. 57-yr-old female with *Fasciola hepatica* infection of the liver. (A) Axial DWI shows a subcapsular tubular area of hyperintense signal in segment 6 (arrow). (B) Axial HASTE with fat sat shows no visible correlate (arrow). (C) and (D) axial and (E) coronal portal venous phase images post-gadoxetic acid injection show the extent of the subcapsular lesion, which appears as “tunnels and caves” (arrows). (F) Axial image, 20 min post-gadoxetic acid injection, shows lack of lesion enhancement (arrow). DWI, diffusion-weighted imaging.

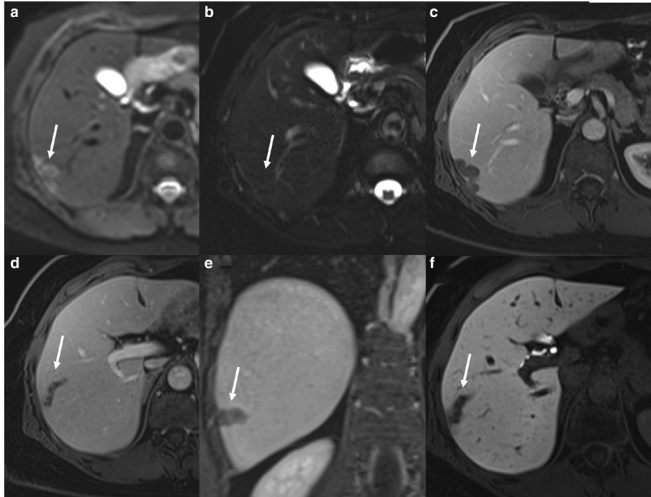
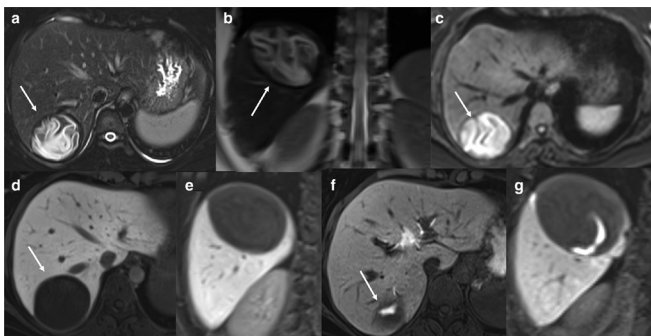


Figure 4. 34-yr-old female with a hepatic hydatid infection. (A) Axial T2-weighted HASTE fat sat show a 6.2 cm cystic lesion with floating, undulating membranes within it due to detached endocysts (daughter cysts) in segment 7 (arrow). (B) Coronal HASTE and (C) Axial DWI (b 300 s/mm<sup>2</sup>) again show the “water-lily sign” of this Echinococcal cyst (arrow). (D) Axial and (E) coronal T1-weighted GRE, 20 min post-gadoxetic acid injection (HBP), show no enhancement within the cyst. (F) Axial and (G) coronal images obtained three hours after injection show enhancement of the lesion (arrow), indicating its communication with the biliary tree. Caveat: Delayed images, *i.e.* 2–3 h after gadoxetic acid injection to determine whether the patient was a candidate for PAIR must be obtained. If no connection to the bile ducts is found, then PAIR can be performed. DWI, diffusion-weighted imaging; HBP, hepatobiliary-phase; PAIR, puncture-aspiration-injection-reaspiration.



*Fasciola hepatica* has a predilection for the right subphrenic space where it can form low-attenuation liver lesions, called “tunnels and caves,” sometimes complicated by hemorrhage and capsular retraction (Figure 3). *Hepatic schistosomiasis* has non-specific imaging findings of cirrhosis.<sup>45</sup>

In *Echinococcus granulosus*, the liver, followed by the lungs, are the most commonly involved organs. Once suspected, MRCP, and T2-weighted MR sequences can give the extent of biliary tree involvement. Like CT, MRI can determine the content and grade of the cysts. A hypointense peripheral rim surrounding a hydatid cyst on T2-weighted images is thought to be due to fibrosis or calcification. However, wall calcification is better seen on CT. Percutaneous drainage has replaced surgical decompression in many instances of parasitic disease.<sup>46</sup> Morbidity, mortality, and recurrence have been shown to be greater the more radical the surgery. Cyst diameters > 7.5 cm are associated with a high risk of bile duct communication.<sup>47</sup> Gadoxetic acid-enhanced MRC in the delayed phase, *i.e.* 2–3 h after injection, is recommended to exclude communication between the cyst and the biliary system before percutaneous ultrasound or CT-guided PAIR (puncture-aspiration-injection-reaspiration) is performed (Figure 4).

#### In immunocompromised patients

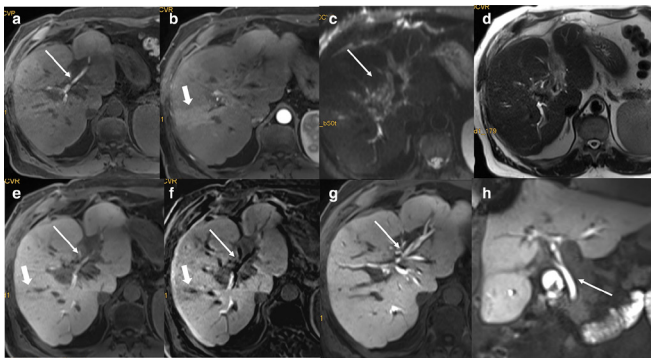
Immunocompromised patients prone to opportunistic infections often develop biliary stricture(s) that lead to cholestatic liver impairment. AIDS cholangiopathy occurs primarily in those with very low CD4 counts, drug-resistant HIV or lack of access to antiretroviral therapy.<sup>48</sup> *Cryptosporidium parvum*, and CMV, the most common inciting pathogens, may cause peri-ampullary stenosis (isolated finding in 10%), “beading” of the IHD resembling sclerosing cholangitis, or segmental EHD strictures with/out IHD involvement, thought to be secondary to ischaemia.<sup>48</sup>

Liver transplant recipients are also prone to cholangitis, typically from biliary infection, chronic rejection, ischaemia, drugs, or anastomotic stricture.<sup>49</sup> Because the biliary tree cholangiocytes (epithelial cells of the bile duct) are supplied by the peribiliary plexus, which comes from the hepatic artery, it is prone to hypoxia compared to the hepatocyte, which receives a dual blood supply, *i.e.* the hepatic artery and the portal vein.<sup>50</sup> Anastomotic or non-anastomotic strictures are best detected by MRCP, which has a sensitivity and specificity of 95%. Non-anastomotic stenoses (NAS) are characterised by intraductal casts and/or intrahepatic biloma formation, requires retransplantation in over 10%<sup>51</sup> (Figure 5). The presence of bile duct-wall necrosis, with spillage of secretions into the liver parenchyma, portends a poor prognosis. On the contrary, if an isolated anastomotic stricture is suspected, ERCP is done so that balloon dilatation and/or stenting can follow, if necessary.

#### Immune-mediated

Autoimmune diseases, plus some drugs and toxins, have been implicated in the development of chronic cholangitis.<sup>1</sup> Because these patients have no or mild symptoms early on, *i.e.* fatigue and pruritus, cholangiocyte and/or hepatocyte damage may already be advanced when they present with elevated cholestatic liver enzymes.<sup>52</sup> What unifies the group of sclerosing cholangitides is their imaging appearance, which resembles that of PSC.

Figure 5. 56-yr-old male with biliary casts after OLT. (A) Axial unenhanced T1 GRE shows a linear hyperintensity along the intrahepatic bile ducts (arrow) indicative of biliary casts. (B) Axial T1 GRE, arterial phase post-gadoxetic acid injection, shows a wedge-shaped peripheral area (arrow) of increased SI in segment 6 of the right liver lobe indicative of segmental cholangitis. (C) Axial DWI ( $b = 300 \text{ s/mm}^2$ ) confirms this wedge-shaped area of cholangitis and shows pronounced periportal tracking (arrow). (D) Axial T2 HASTE shows slightly dilated intrahepatic bile ducts predominantly in the right lobe. (E) Axial T1 GRE, 20 min post-gadoxetic acid injection (HBP), and F,) subtraction image, show no contrast excretion from the left biliary system (thin arrow), as well as the hypointense wedge-shaped area of cholangitis (thick arrow) in the right liver lobe due to partial obstruction of biliary cast. (G) Axial and H) coronal T1 GRE, 2 h post-gadoxetic acid injection, finally show opacification of the left biliary system (arrow), the CBD (arrow), and the duodenum due to biliary casts that were partially obstructive. CBD, common bile duct; DWI, diffusion-weighted imaging; HBP, hepatobiliary-phase; OLT, orthotopic liver transplantation.



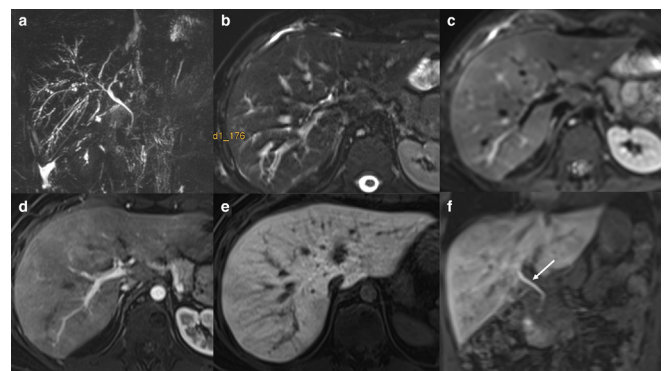
Intraductal filling defects, representing casts, sludge, and/or stones, may be present.

### Secondary sclerosing cholangitis (SSC)

The most frequent chronic cholestatic disease is sclerosing cholangitis (SC), due to bile duct inflammation, obliterative fibrosis, and stricture formation that can end in liver cirrhosis.<sup>53</sup> SC can be classified as primary (PSC) and secondary sclerosing cholangitis (SSC). Because PSC is a diagnosis of exclusion, comprising those patients with imaging findings of sclerosing cholangitis, but an unknown cause, we will start with SSC.<sup>53</sup> The imaging features of SSC are identical to those of PSC, including multiple short-segment strictures with intervening normal-calibre or slightly dilated segments, which results in a beaded appearance (Figure 6).

Causes linked to SC include infection, immune-mediated injury (suggested by elevated IgG4 serum levels and/or lymphocytic infiltrates at histology), ischaemia, toxins, recurrent pancreatitis, Langerhans cell histiocytosis, and mastocytosis, as well as untreated mechanical biliary obstruction that progresses over time.<sup>53–55</sup> However, iatrogenic causes are among the most frequently reported, including surgical trauma or ischaemic injury after orthotopic liver transplantation (OLT),<sup>56</sup> and intra-arterial chemotherapy.<sup>57</sup> Recently, a largely unrecognised new

Figure 6. 20-yr-old male with secondary sclerosing cholangitis who spent many months in the ICU due to a stroke. (A) Coronal MRCP T2-weighted MIP shows diffuse corkscrew irregularity of the intrahepatic biliary tree with strictures and dilatations. (B) Axial T2 HASTE fat sat shows predominantly right intrahepatic bile duct dilatation. (C) Axial DWI ( $b = 300 \text{ s/mm}^2$ ) shows periportal tracking and multiple, patchy, faint hyperintense areas of segmental cholangitis. (D) Axial T1 GRE, arterial phase post-gadoxetic acid injection, shows inhomogeneous parenchymal liver enhancement. (E) Axial and F) coronal GRE, 20 min post-gadoxetic acid injection (HBP), confirm the inhomogeneous parenchymal contrast enhancement, diminished especially in the right liver lobe due to chronic cholangitis. However, liver function is preserved, with timely hepatobiliary excretion (arrow). ICU, intensive care unit; HBP, hepatobiliary-phase; MIP, maximum intensity projection; MRCP, magnetic resonance cholangiopancreatography.



form of SSC, also believed to be due to ischaemia and/or systemic inflammation, has been observed in intensive care unit patients. Referred to as SSC-CIP (critically ill patients), they typically have sepsis, shock, trauma, and burns.<sup>58</sup> The hallmark of SSC-CIP is the early formation of biliary casts.<sup>53</sup> Sometimes the diagnosis can be made by portable ultrasound, especially if patients are unstable. Biliary casts may be overlooked early but as the mixture of inspissated bile and sloughed biliary mucosa hardens, it can appear as linear highly echogenic debris within alternating dilated and strictured bile ducts. Diagnosis often requires ERCP which may also allow attempts to remove biliary casts and debris. Rapid progression to liver cirrhosis, with a median survival of 13 months without OLT, is their typical fate.<sup>58</sup> Recently, post-COVID-19 cholangiopathy, with clinical and histologic features similar to SSC, was reported in three patients. It is thought to be due to direct viral cholangiocyte injury,<sup>59,60</sup> with possible overlapping pathogenetic hypoxia and cytokine storm. Therapeutic options for most forms of SSC are limited. Patients who do not undergo OLT have significantly reduced survival compared to PSC patients.<sup>61</sup>

### Primary sclerosing cholangitis (PSC)

Primary sclerosing cholangitis (PSC) is a rare, chronic, progressive immune-mediated inflammatory disease predominantly in middle-aged males, of whom over 70% also have inflammatory bowel disease (IBD).<sup>1</sup> Usually asymptomatic, the diagnosis is made by elevated alkaline phosphatase ( $\geq 6$  months),<sup>1</sup> screening MRCP for stricture detection, and the absence of any

Figure 7. 42-yr-old male with chronic inflammatory bowel disease and elevated cholestatic liver enzymes due to PSC. (A) Axial DWI ( $b = 300 \text{ s/mm}^2$ ) shows a wedge-shaped peripheral area of increased SI in segment 6 (arrow) of the right liver lobe. (B) Axial T1 GRE, arterial phase post-gadoxetic acid injection, shows wedge-shaped enhancement in segment 6 (arrow). (C) Axial and (D) coronal T1 GRE, 20 min post-gadoxetic acid injection (HBP), show absent enhancement in the wedge-shaped area of cholangitis (arrow) indicative of early PSC. Strong uniform liver enhancement and timely contrast excretion indicate the preservation of liver function. DWI, diffusion-weighted imaging; HBP, hepatobiliary-phase; PSC, primary sclerosing cholangitis; SI, signal intensity.

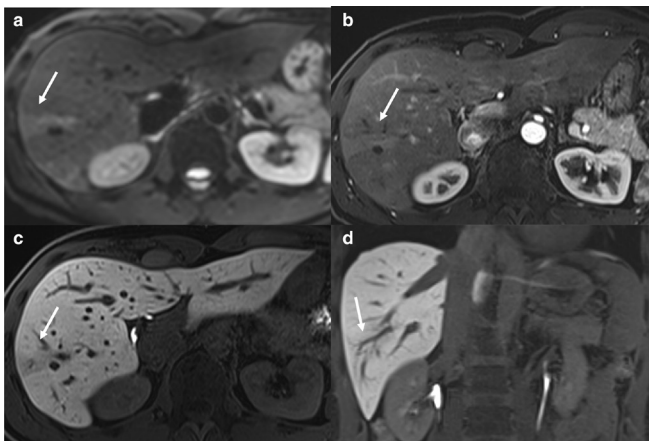
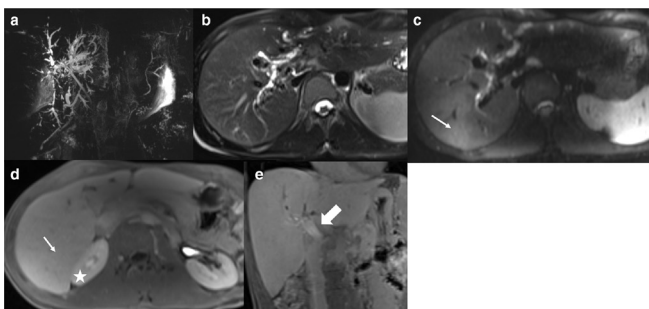


Figure 8. 26-yr-old male with chronic inflammatory bowel disease and advanced PSC. (A) Coronal MRCP T2-weighted MIP shows multiple segmental strictures alternating with dilated segments of the more central biliary tree, the so called “beads-on-a-string” appearance, and the absence of bile ducts peripherally; in other words, an incipient form of a “pruned tree.” (B) Axial HASTE fat sat shows dilatation of predominantly the central intrahepatic bile ducts. (C) Axial DWI ( $b = 300 \text{ s/mm}^2$ ) shows biliary dilatation and faint areas of segmental cholangitis (arrow). (D) Axial and (E) coronal T1 GRE, 20 min post-gadoxetic acid injection (HBP), show uniformly decreased enhancement of the liver (thin arrow) relative to the right kidney (asterisk) and mild enhancement, *i.e.*, contrast retention, in the portal vein (thick arrow) indicating absent hepatobiliary excretion (*i.e.*, FLIS = 0). A few months later, the patient received a liver transplant. HBP, hepatobiliary-phase; MIP, maximum intensity projection; MRCP, magnetic resonance cholangiopancreatography; PSC, primary sclerosing cholangitis.



risk factors for SSC.<sup>62</sup> Although 90% of patients have classic PSC, involving the entire biliary tree, 5% have exclusively small-duct pathology, *i.e.* involving the peripheral IHD, which has no imaging correlate,<sup>63</sup> or overlap syndrome, which describes concurrent autoimmune hepatitis (AIH) and PSC.<sup>64</sup> Only in these two instances a liver biopsy is necessary for diagnosis.<sup>65</sup> Periductal onion-skin-like fibrosis on histology confirms the diagnosis, though this finding is seen in only 10–20%,<sup>65</sup> likely due to the performance of blind biopsy within unevenly distributed disease. Gadoxetic acid-enhanced MRI and DWI can detect early or subtle PSC, potentially guiding the biopsy (Figure 7).<sup>66</sup>

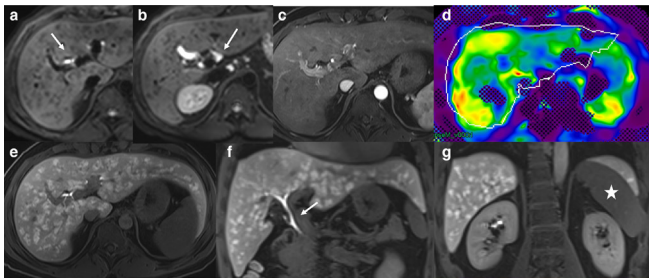
Due to the lack of established drug therapy for PSC, OLT is the only curative treatment, although many centers use Ursodeoxycholic acid (UDCA) despite an unproven survival benefit in PSC.<sup>1</sup> However, annual CA 19–9 and MRCP are recommended for CCA, and ultrasound for gallbladder cancer surveillance.<sup>1</sup> Furthermore, in PSC patients with IBD, the risk of colon cancer increases fourfold over patients with solely IBD which justifies (bi)annual surveillance colonoscopy. Serial LFTs determine the timing of MRCP and MRI to screen for the development of a dominant stricture (DS), the severity of which serves as a prognosticator.<sup>67</sup> Functional imaging with gadoxetic acid-enhanced MRI is the non-invasive method of choice.<sup>40</sup> The appearance of gadoxetic acid within the expected 20 min of injection, *i.e.* the HB phase image, indicates that the stricture under evaluation is of no functional significance.<sup>68</sup> When excretion exceeds 20 min, we consider the possibility of a DS, warranting dilatation with ERCP. Caveat: If morphologic features of advanced cirrhosis are present, delayed excretion could be due to chronically impaired function.<sup>69</sup> Endoscopic biopsies (to exclude CCA) and dilatation with and without short-term stenting of such DS is essential to PSC management.<sup>70</sup> In addition, parenchymal progression to liver cirrhosis can be followed on serial MRIs, both dynamic and DWI. In advanced PSC, gadoxetic acid-enhanced MRI aids pre-OLT evaluation and post-OLT follow-up, including graft injury and disease recurrence (Figure 8).<sup>69,71,72</sup> Recently, Bastati et al introduced the so-called FLIS score as a semiquantitative method with which to predict survival in chronic liver disease and liver transplant patients.<sup>69,72</sup>

### Primary biliary cholangitis (PBC)

Initially called primary biliary cirrhosis (PBC), the name was recently changed to group it among the cholangitides, and to raise awareness that cirrhosis can be prevented by treatment, particularly during earlier stages. PBC predominantly affects females over 40 years of age.<sup>1</sup> Of autoimmune origin, it usually occurs with conditions such as Hashimoto’s thyroiditis, Sjogren’s disease, or celiac disease. Although the antimicrobial antibody (AMA) test is not specific for PBC, over 90% of PBC patients will be AMA-positive and another 30% positive for the PBC-unique antinuclear antibodies (ANA, directed against gp210 or sp100, usually allowing a diagnosis without liver biopsy).<sup>73</sup>

On ultrasound or cross-sectional imaging, there are no characteristic findings in early PBC, other than occasional porta hepatis or gastroduodenal ligament lymphadenopathy.<sup>74</sup> Although the main role of MRI is to exclude other causes of IHD or EHD

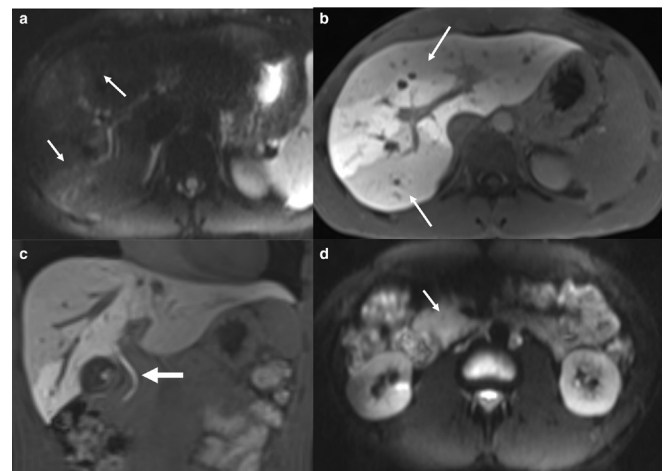
Figure 9. 34-yr-old male with advanced primary biliary cholangitis. (A) and (B) Axial DWI ( $b = 300 \text{ s/mm}^2$ ) show periportal tracking (arrow), (A) and increased lymph nodes in the hepatoduodenal ligament (arrow), (B)). (C) Axial T1 GRE, arterial phase post-gadoxetic acid injection, shows no significant abnormalities. (D) Axial MR-Elastography map shows significantly increased liver stiffness values, approximately 3.5 kPa compatible with Stage 3 fibrosis. (E) Axial and (F) and (G) coronal T1 GRE, 20 min post-gadoxetic acid injection (HBP), show inhomogeneous uptake with multiple high SI intraparenchymal nodules compatible with RNH. Prompt hepatobiliary excretion (arrow) indicates preserved liver function. Increased longitudinal diameter of the spleen is due to splenomegaly (asterisk). HBP, hepatobiliary-phase; RNH, regenerative nodular hyperplasia.



cholangitis, lymphadenopathy and periportal tracking, defined as linear high-SI on T2-weighted images that parallel the bile duct walls, are frequent findings.<sup>74</sup> Histology (when obtained) confirms that this “tracking” corresponds to active inflammation in the portal tracts, meaning that its presence can be used to assess disease activity.<sup>75</sup> The fact that periportal tracking is absent in late-stage disease supports that it is a marker of acute inflammation.<sup>76</sup> Additional imaging findings include signs of portal hypertension, which may also be seen in pre-cirrhotic stages, possibly caused by a pre-sinusoidal block at the level of the portal tract, granuloma formation, ductal proliferation, and pronounced portal fibrosis.<sup>76</sup> Interestingly, splenomegaly is much greater in the early stages of PBC than in end-stage disease.<sup>77</sup> Although lymphadenopathy has been seen in 80% of PBC patients on CT, neither it, periportal tracking, nor splenomegaly are unique to PBC. The diagnosis of PBC relies on elevated cholestatic liver enzymes and the presence of AMA and/or PBC-specific ANA.<sup>1</sup> Diagnostic liver biopsy is necessary when these two antibodies are absent.<sup>73</sup>

UDCA is the mainstay of therapy in these patients since disease is primarily limited to the small IHDs. Biochemical response to UDCA after 12 months, and various scores (e.g. GLOBE, UK-PBC score) are important prognostic factors that guide therapy with initiation of second line therapy (obetocholic acid, fibrates) in incomplete responders to UDCA.<sup>73</sup> The liver volume (LV) to splenic volume (SV) ratio is an important prognosticator in PBC. A low LV/SV ratio is associated with a significantly poorer outcome in PBC patients. Moreover, the LV/SV ratio was found to be significantly lower in PBC patients who developed symptoms than in those who remained asymptomatic.<sup>78</sup> Furthermore, spleen and liver stiffness measurements, obtained

Figure 10. 22-yr-old male presented with acute abdominal pain and clinical suspicion of pancreatitis. He had elevated serum enzymes in the course of IgG4-related sclerosing cholangitis. (A) Axial DWI ( $b = 300 \text{ s/mm}^2$ ) shows multiple, wedge-shaped, peripheral areas of increased SI in both liver lobes (arrows) consistent with segmental cholangitis. (B) Axial and (C) coronal T1 GRE, 20 min post-gadoxetic acid injection (HBP), show poor enhancement of the areas corresponding to high SI on DWI (arrows), which confirmed regional liver impairment due to segmental cholangitis. Timely excretion (thick arrow) indicates that function was preserved. (D) Axial DWI ( $b = 300 \text{ s/mm}^2$ ) shows a diffusely thickened high-signal-intensity area, corresponding to the oedematous pancreatic head (arrow) due to AIP in the spectrum of IgG4 disease. AIP, autoimmune pancreatitis; DWI, diffusion-weighted imaging; HBP, hepatobiliary-phase; SI, signal intensity.



by transient elastography, are excellent markers for advanced disease, *i.e.* advanced fibrosis or cirrhosis<sup>73</sup> (Figure 9).

Again, OLT is the only curative treatment for end-stage PBC. However, on average, 20% of these patients will have clinical manifestations of recurrent PBC, although the rate of histological recurrence is likely higher.<sup>79</sup> As AMA titers remain positive post-OLT, liver histology is necessary to diagnose recurrent PBC. In contrast to PSC, it is rather uncommon for recurrent PBC to lead to graft failure since continuing UDCA therapy significantly reduces the risk of recurrence.<sup>80</sup>

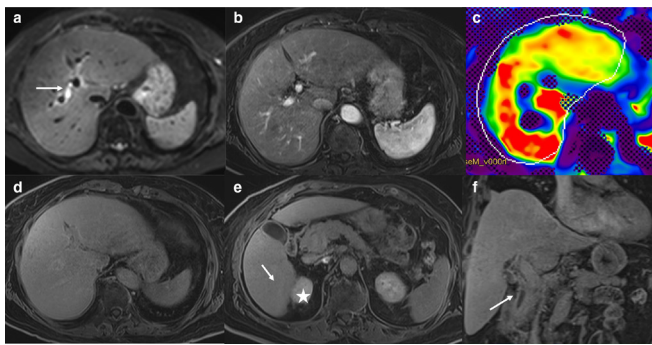
As in PSC, MRI plays an important role in following biliary cirrhosis, excluding acute mechanical obstruction should LFTs suddenly rise. Although overlap syndrome, *i.e.* simultaneous AIH and PBC, could explain such laboratory results, PBC patients are subject to choledocholithiasis as in other middle-aged females. Furthermore, HCC must be considered, especially in males. Surveillance is part of PBC management.<sup>81</sup>

#### IgG4-related sclerosing cholangitis

IgG4-related sclerosing cholangitis is one manifestation of this systemic immune-mediated inflammatory entity that can affect multiple organs over time.<sup>82,83</sup> Although serology may show elevated titers, this is not sufficient for diagnosis since elevated serum IgG4 levels can also occur with malignancies, such as



Figure 11. 75-yr-old psoriatic female with drug-induced cholestasis after Ixekizumab. (A) Axial DWI ( $b = 300 \text{ s/mm}^2$ ) shows mildly increased SI diffusely in the liver due to oedema and periportal tracking (arrow). (B) Axial T1 GRE, arterial phase post-gadoxetic acid injection, is unremarkable. (C) Axial MR-Elastography map shows significantly increased liver stiffness values, approximately 4.5 kPa, indicative of diffuse oedema due to DILI. (D), (E) Axial and (F) coronal T1 GRE, 20 min post-gadoxetic acid injection (HBP), show markedly reduced contrast media uptake (thin arrow), (E) relative to the right kidney (asterisk), (E) and absent hepatobiliary excretion (thin arrow), (F) indicating very poor liver function. The patient recovered weeks after drug cessation, indicating that DILI was transient and reversible. DILI, drug-induced liver injury; DWI, diffusion-weighted imaging; HBP, hepatobiliary-phase.



pancreatic adenocarcinoma and lymphoma. However, IgG4 disease is very likely when serum IgG4 levels exceed the upper limits of normal by fourfold.<sup>84</sup> Definitive diagnosis is made using the HISORt criteria which are based upon imaging findings, serology, response to steroid therapy, and, most importantly, histology.<sup>82</sup> The role of imaging is to exclude IgG4 mimickers, especially underlying malignancy.<sup>85</sup> In the early stages of IgG4 disease, ultrasound is usually normal. Subsequently, however, gallbladder and bile duct wall thickening anywhere, with or without IHD dilatation, may be seen. These findings are confirmed on cross-sectional imaging.<sup>86</sup> In particular, MR shows smooth wall thickening that results in single or multifocal, long-segment stricture(s), restriction on DWI, and delayed homogeneous contrast enhancement (Figure 10). The differential diagnosis of Klatskin tumour or pancreatic cancer must be considered when inflammatory pseudotumour of the hilar ducts or the pancreatic head, *i.e.* mass-like thickening, occurs.<sup>87,88</sup> Immunosuppression with steroid therapy is considered the first-line treatment of IgG4-related disease, but the risk of recurrence is high, requiring long-term immunosuppression (azathioprine) or other B-cell-depleting strategies, such as rituximab.<sup>89</sup>

#### Miscellaneous

Approximately, 30% of patients with drug-induced liver injury (DILI) show serum LFTs consistent with cholestatic disease. While most mechanisms of drug-induced cholestasis involve hepatocellular cholestasis, some drugs, *e.g.* anti-seizure medications like phenobarbital and carbamazepine, can cause immune-mediated destruction of the biliary epithelium and interlobular ducts.<sup>90</sup> Histology shows a pattern of inflammation and necrosis

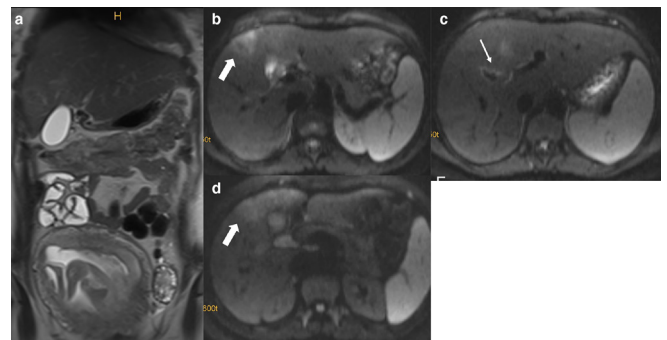
similar to that seen in PBC, and eosinophils may suggest a drug aetiology. A few drugs, such as the fluorodeoxyuridines and 5-fluorouracil, can cause large-duct injury (*e.g.* the common hepatic or perihilar intrahepatic bile ducts) with features resembling PSC.<sup>90,91</sup> Therefore, diagnosis primarily rests on a careful medication history and histologic findings.<sup>92</sup>

MR is the most sensitive imaging modality for DILI, particularly when DWI and gadoxetic acid-enhanced T1-weighted sequences are obtained. There may be evidence of periportal tracking, reduced uptake, and absent excretion of gadoxetic acid in the hepatobiliary phase as small ducts disappear, *i.e.* vanishing duct syndrome (Figure 11). CT and ultrasound show non-specific findings of liver injury, including hepatomegaly and heterogeneously enhancing parenchyma. When injury is severe, fibrosis and cirrhosis can be seen.<sup>93</sup>

Chemotherapy-induced sclerosing cholangitis (CISC) is a frequent, potentially fatal complication of hepatic arterial infusion chemotherapy, occurring in up to 50% of patients being treated for hepatobiliary malignancies. The resulting biliary stricture may result in progressive cholangitis, unless recognised and treated early.<sup>94</sup>

In athletes and body builders, anabolic steroid use should be considered if an otherwise healthy adult presents with unexplained cholestasis. The spectrum of imaging findings is non-specific, ranging from chronic hepatitis to vascular injury to bile duct damage. Although, anabolic-induced cholestasis starts with pure hepatocellular cholestasis, severe ductopenia, known as vanishing duct syndrome, may be seen on histology in chronic cases. As this is not specific for anabolic steroids, the diagnosis

Figure 12. 23-yr-old admitted with hyperemesis gravidarum and upper abdominal pain in week 24 of pregnancy. Gastroscopy was unremarkable. MRI was then performed to exclude mechanical biliary obstruction. Final diagnosis was antiphospholipid syndrome, as well as ICP. (A) Coronal HASTE demonstrates a third-trimester pregnancy. (B, C) and (D) Axial DWI ( $b = 300 \text{ s/mm}^2$ ) show an extended wedge-shaped area peripherally (thick arrows) of increased SI predominantly in segment IVa and IVb, plus periportal tracking (thin arrow) indicative of pregnancy-induced cholestasis and segmental cholangitis. Following delivery, the patient's pruritus resolved and liver function tests returned to normal. DWI, diffusion-weighted imaging; ICP, intrahepatic cholestasis/cholangitis of pregnancy; SI, signal intensity.



is presumptive, based on improvement following cessation of steroids. However, if severe enough, the patient can present in acute liver failure.<sup>95</sup>

Transient intrahepatic cholestasis of pregnancy (ICP), in 0.2% of females, usually occurs during the second and third trimesters. Typically treated with antipruritics, these patients almost never come to imaging. We present a case where ICP was incidentally noted in a patient who underwent MRI for unexplained hyperemesis gravidarum in week 24 of pregnancy and elevated LFTs to exclude mechanical obstruction. The final diagnosis was anti-phospholipid syndrome (Figure 12).

Stauffer syndrome should be kept in mind in the cancer patient with unexplained cholestasis. The underlying malignancy is the clue to the imaging diagnosis. Interleukin six causes cholestasis in the absence of biliary obstruction or infiltration through the tumour.

Graft versus host disease (GVHD) may cause hepatocyte and/or cholangiocyte necrosis and cell death in allogeneic more often than autologous stem cell transplant recipients. Since imaging features and histologic inflammatory infiltrates are nonspecific, the clue to the diagnosis is the presence of concurrent skin and intestinal findings, as well as the timing of elevated serum LFTs. GVHD typically starts within weeks of transplantation, even sooner without immunosuppression.<sup>96</sup>

## SUMMARY

Imaging plays a crucial role in the diagnosis of acute and chronic cholangitis. Ultrasound is usually the initial investigation. CT is helpful in the evaluation of trauma, oncologic, or post-operative complications. Conventional T2-weighted MRCP is the most helpful diagnostic modality, despite some shortcomings. DWI and gadoteric acid-enhanced MRC can overcome these limitations, further detecting liver parenchymal damage, which is an indicator of early biliary disease, and predicting survival.

## REFERENCES

- European association for the study of the L. EASL clinical practice guidelines: management of cholestatic liver diseases. *J Hepatol* 2009; **51**: 237–67.
- Azizi L, Raynal M, Cazejust J, Ruiz A, Menu Y, Arrivé L. Mr imaging of sclerosing cholangitis. *Clin Res Hepatol Gastroenterol* 2012; **36**: 130–8. doi: <https://doi.org/10.1016/j.clinre.2011.11.011>
- Lan Cheong Wah D, Christophi C, Muralidharan V. acute cholangitis: current concepts. *ANZ J Surg* 2017; **87**(7-8): 554–9.
- Tsunezama K, Kono N, Yamashiro M, Kouda W, Sabit A, Sasaki M, et al. Aberrant expression of stem cell factor on biliary epithelial cells and peribiliary infiltration of c-kit-expressing mast cells in hepatolithiasis and primary sclerosing cholangitis: a possible contribution to bile duct fibrosis. *J Pathol* 1999; **189**: 609–14. doi: [https://doi.org/10.1002/\(SICI\)1096-9896\(199912\)189:4<609::AID-PATH474>3.0.CO;2-2](https://doi.org/10.1002/(SICI)1096-9896(199912)189:4<609::AID-PATH474>3.0.CO;2-2)
- Marin JJG, Macias RIR, Briz O, Banales JM, Monte MJ. Bile acids in physiology, pathology and pharmacology. *Curr Drug Metab* 2015; **17**: 4–29. doi: <https://doi.org/10.2174/1389200216666151103115454>
- Hofmann AF. Bile acid secretion, bile flow and biliary lipid secretion in humans. *Hepatology* 1990; **12**(Pt 2): 17S–22.
- Trauner M, Meier PJ, Boyer JL. Molecular pathogenesis of cholestasis. *N Engl J Med* 1998; **339**: 1217–27. doi: <https://doi.org/10.1056/NEJM199810223391707>
- Sulzer JK, Ocun LM. Cholangitis: causes, diagnosis, and management. *Surg Clin North Am* 2019; **99**: 175–84. doi: <https://doi.org/10.1016/j.suc.2018.11.002>
- Ahmed M. Acute cholangitis - an update. *World J Gastrointest Pathophysiol* 2018; **9**: 1–7. doi: <https://doi.org/10.4291/wjgp.v9.i1.1>
- Wada K, Takada T, Kawarada Y, Nimura Y, Miura F, Yoshida M, et al. Diagnostic criteria and severity assessment of acute cholangitis: Tokyo guidelines. *J Hepatobiliary Pancreat Surg* 2007; **14**: 52–8. doi: <https://doi.org/10.1007/s00534-006-1156-7>
- Ely R, Long B, Koefman A. The emergency Medicine-Focused review of cholangitis. *J Emerg Med* 2018; **54**: 64–72. doi: <https://doi.org/10.1016/j.jemermed.2017.06.039>
- Okabayashi T, Shima Y, Sumiyoshi T, Sui K, Iwata J, Morita S, et al. Incidence and risk factors of cholangitis after hepaticojejunostomy. *J Gastrointest Surg* 2018; **22**: 676–83. doi: <https://doi.org/10.1007/s11605-017-3532-9>
- Sokal A, Sauvanet A, Fantin B, de Lastours V. Acute cholangitis: diagnosis and management. *J Visc Surg* 2019; **156**: 515–25. doi: <https://doi.org/10.1016/j.jvisc.2019.05.007>
- Oku T, Maeda M, Waga E, Wada Y, Nagamachi Y, Fujita M, et al. Cytomegalovirus cholangitis and pancreatitis in an immunocompetent patient. *J Gastroenterol* 2005; **40**: 987–92. doi: <https://doi.org/10.1007/s00535-005-1683-z>
- Jüngst C, Lammert F. Cholestatic liver disease. *Dig Dis* 2013; **31**: 152–4. doi: <https://doi.org/10.1159/000347210>
- Ker CG, Chen JS, Lee KT, Sheen PC, Wu CC. Assessment of serum and bile levels of CA19-9 and CA125 in cholangitis and bile duct carcinoma. *J Gastroenterol Hepatol* 1991; **6**: 505–8. doi: <https://doi.org/10.1111/j.1440-1746.1991.tb00896.x>
- Kim S, Park BK, Seo JH, Choi J, Choi JW, Lee CK, et al. Carbohydrate antigen 19-9 elevation without evidence of malignant or pancreatobiliary diseases. *Sci Rep* 2020; **10**: 8820. doi: <https://doi.org/10.1038/s41598-020-65720-8>
- Narimatsu H, Iwasaki H, Nakayama F, Ikehara Y, Kudo T, Nishihara S, et al. Lewis and secretor gene dosages affect CA19-9 and DU-PAN-2 serum levels in normal individuals and colorectal cancer patients. *Cancer Res* 1998; **58**: 512–8.
- O'Connor OJ, O'Neill S, Maher MM. Imaging of biliary tract disease. *AJR Am J Roentgenol* 2011; **197**: W551–8. doi: <https://doi.org/10.2214/AJR.10.4341>
- Benarroch-Gampel J, Boyd CA, Sheffield KM, Townsend CM, Riall TS. Overuse of CT in patients with complicated gallstone disease. *J Am Coll Surg* 2011; **213**: 524–30. doi: <https://doi.org/10.1016/j.jamcollsurg.2011.07.008>
- Walas MK, Skoczylas K, Gierbliński I. Errors and mistakes in the ultrasound diagnostics of the liver, gallbladder and bile ducts. *J Ultrason* 2012; **12**: 446–62. doi: <https://doi.org/10.15557/JoU.2012.0032>
- Válek V, Kala Z, Kysela P. Biliary tree and cholecyst: post surgery imaging. *Eur J Radiol* 2005; **53**: 433–40. doi: <https://doi.org/10.1016/j.ejrad.2004.12.014>
- Yeh BM, Liu PS, Soto JA, Corvera CA, Hussain HK. Mr imaging and CT of the

- biliary tract. *Radiographics* 2009; **29**: 1669–88. doi: <https://doi.org/10.1148/rg.296095514>
24. Salvolini L, Urbinati C, Valeri G, Ferrara C, Giovagnoni A. Contrast-Enhanced Mr cholangiography (MRCP) with GD-EOB-DTPA in evaluating biliary complications after surgery. *Radiol Med* 2012; **117**: 354–68. doi: <https://doi.org/10.1007/s11547-011-0731-4>
  25. Tamrazi A, Vasanawala SS. Functional hepatobiliary MR imaging in children. *Pediatr Radiol* 2011; **41**: 1250–8. doi: <https://doi.org/10.1007/s00247-011-2086-3>
  26. Mosler P. Diagnosis and management of acute cholangitis. *Curr Gastroenterol Rep* 2011; **13**: 166–72. doi: <https://doi.org/10.1007/s11894-010-0171-7>
  27. Schneider J, Hapfelmeier A, Thöres S, Obermeier A, Schulz C, Pörringer D, et al. Mortality risk for acute cholangitis (MAC): a risk prediction model for in-hospital mortality in patients with acute cholangitis. *BMC Gastroenterol* 2016; **16**: 15. doi: <https://doi.org/10.1186/s12876-016-0428-1>
  28. Moole H, Bechtold M, Puli SR. Efficacy of preoperative biliary drainage in malignant obstructive jaundice: a meta-analysis and systematic review. *World J Surg Oncol* 2016; **14**: 182. doi: <https://doi.org/10.1186/s12957-016-0933-2>
  29. Yokoe M, Hata J, Takada T, Strasberg SM, Asbun HJ, Wakabayashi G, et al. Tokyo guidelines 2018: diagnostic criteria and severity grading of acute cholecystitis (with videos). *J Hepatobiliary Pancreat Sci* 2018; **25**: 41–54. doi: <https://doi.org/10.1002/jhbp.515>
  30. Karlsen TH, Folseraas T, Thorburn D, Vesterhus M. Primary sclerosing cholangitis - a comprehensive review. *J Hepatol* 2017; **67**: 1298–323. doi: <https://doi.org/10.1016/j.jhep.2017.07.022>
  31. Raper SE, Barker ME, Jones AL, Way LW. Anatomic correlates of bacterial cholangiovenous reflux. *Surgery* 1989; **105**: 352–9.
  32. Jeong SW, Jang JY, Lee TH, Kim HG, Hong SW, Park SH, et al. Cryptogenic pyogenic liver abscess as the herald of colon cancer. *J Gastroenterol Hepatol* 2012; **27**: 248–55. doi: <https://doi.org/10.1111/j.1440-1746.2011.06851.x>
  33. Beliaev AM, Zyl'korneeva Sof'ya, Rowbotham D, Bergin CJ. Screening acute cholangitis patients for sepsis. *ANZ J Surg* 2019; **89**: 1457–61. doi: <https://doi.org/10.1111/ans.15432>
  34. See TC. Acute biliary interventions. *Clin Radiol* 2020; **75**: 398.e9–398.e18. doi: <https://doi.org/10.1016/j.crad.2019.03.012>
  35. Melamud K, LeBedis CA, Anderson SW, Soto JA. Biliary imaging: multimodality approach to imaging of biliary injuries and their complications. *Radiographics* 2014; **34**: 613–23. doi: <https://doi.org/10.1148/rg.343130011>
  36. Kim SW, Shin HC, Kim IY. Transient arterial enhancement of the hepatic parenchyma in patients with acute cholangitis. *J Comput Assist Tomogr* 2009; **33**: 398–404. doi: <https://doi.org/10.1097/RCT.0b013e318186faa1>
  37. Catalano OA, Sahani DV, Forcione DG, Czermak B, Liu C-H, Soricelli A, et al. Biliary infections: spectrum of imaging findings and management. *Radiographics* 2009; **29**: 2059–80. doi: <https://doi.org/10.1148/rg.297095051>
  38. Kovač JD, Ješić R, Stanisavljević D, Kovač B, Maksimovic R. Mr imaging of primary sclerosing cholangitis: additional value of diffusion-weighted imaging and ADC measurement. *Acta Radiol* 2013; **54**: 242–8. doi: <https://doi.org/10.1177/0284185112471792>
  39. Fruehwald-Pallamar J, Bastati-Huber N, Fakhrai N, Jantsch M, Puchner S, Herneth AM, et al. Confident non-invasive diagnosis of pseudolesions of the liver using diffusion-weighted imaging at 3T MRI. *Eur J Radiol* 2012; **81**: 1353–9. doi: <https://doi.org/10.1016/j.ejrad.2011.03.072>
  40. Nolz R, Asenbaum U, Schoder M, Wibmer A, Einspieler H, Prusa AM, et al. Diagnostic workup of primary sclerosing cholangitis: the benefit of adding gadoteric acid-enhanced T1-weighted magnetic resonance cholangiography to conventional T2-weighted magnetic resonance cholangiography. *Clin Radiol* 2014; **69**: 499–508. doi: <https://doi.org/10.1016/j.crad.2013.12.008>
  41. Lardièrre-Deguelte S, Ragot E, Amroun K, Piardi T, Dokmak S, Bruno O, et al. Hepatic abscess: diagnosis and management. *J Visc Surg* 2015; **152**: 231–43. doi: <https://doi.org/10.1016/j.jvisurg.2015.01.013>
  42. García-Gutiérrez M, Luque-Márquez R, Rodríguez-Suárez S. Portal vein thrombosis associated with biliary tract infection. *Gastroenterol Hepatol* 2012; **35**: 644–8. doi: <https://doi.org/10.1016/j.gastrohep.2012.03.011>
  43. Lee NK, Kim S, Lee JW, Kim CW, Kim GH, Kang DH, et al. Discrimination of suppurative cholangitis from nonsuppurative cholangitis with computed tomography (CT). *Eur J Radiol* 2009; **69**: 528–35. doi: <https://doi.org/10.1016/j.ejrad.2007.11.031>
  44. Kwan KEL, Shelat VG, Tan CH. Recurrent pyogenic cholangitis: a review of imaging findings and clinical management. *Abdom Radiol* 2017; **42**: 46–56. doi: <https://doi.org/10.1007/s00261-016-0953-y>
  45. Carpenter HA. Bacterial and parasitic cholangitis. *Mayo Clin Proc* 1998; **73**: 473–8. doi: [https://doi.org/10.1016/S0025-6196\(11\)63734-8](https://doi.org/10.1016/S0025-6196(11)63734-8)
  46. Tinsley B, Abbara A, Kadaba R, Sheth H, Sandhu G. Spontaneous intraperitoneal rupture of a hepatic hydatid cyst with subsequent anaphylaxis: a case report. *Case Reports Hepatol* 2013; **2013**: 1–4. doi: <https://doi.org/10.1155/2013/320418>
  47. Rinaldi F, Brunetti E, Neumayr A, Maestri M, Goblrirsch S, Tamarozzi F. Cystic echinococcosis of the liver: a primer for hepatologists. *World J Hepatol* 2014; **6**: 293–305. doi: <https://doi.org/10.4254/wjh.v6.i5.293>
  48. Naseer M, Dailey FE, Juboori AA, Samiullah S, Tahan V, Epidemiology TV. Epidemiology, determinants, and management of AIDS cholangiopathy: a review. *World J Gastroenterol* 2018; **24**: 767–74. doi: <https://doi.org/10.3748/wjg.v24.i7.767>
  49. Yao S, Yagi S, Nagao M, Uozumi R, Iida T, Iwamura S, et al. Etiologies, risk factors, and outcomes of bacterial cholangitis after living donor liver transplantation. *Eur J Clin Microbiol Infect Dis* 2018; **37**: 1973–82. doi: <https://doi.org/10.1007/s10096-018-3333-4>
  50. Gaudio E, Franchitto A, Pannarale L, Carpino G, Alpini G, Francis H, et al. Cholangiocytes and blood supply. *World J Gastroenterol* 2006; **12**: 3546–52. doi: <https://doi.org/10.3748/wjg.v12.i22.3546>
  51. Valls C, Alba E, Cruz M, Figueras J, Andía E, Sanchez A, et al. Biliary complications after liver transplantation: diagnosis with Mr cholangiopancreatography. *AJR Am J Roentgenol* 2005; **184**: 812–20. doi: <https://doi.org/10.2214/ajr.184.3.01840812>
  52. Palmela C, Peerani F, Castaneda D, Torres J, Itzkowitz SH. Inflammatory bowel disease and primary sclerosing cholangitis: a review of the phenotype and associated specific features. *Gut Liver* 2018; **12**: 17–29. doi: <https://doi.org/10.5009/gnl16510>
  53. Ruemmele P, Hofstaedter F, Gelbmann CM. Secondary sclerosing cholangitis. *Nat Rev Gastroenterol Hepatol* 2009; **6**: 287–95. doi: <https://doi.org/10.1038/nrgastro.2009.46>
  54. Thompson HH, Pitt HA, Lewin KJ, Longmire WP. Sclerosing cholangitis and histiocytosis X. *Gut* 1984; **25**: 526–30. doi: <https://doi.org/10.1136/gut.25.5.526>
  55. Abdalian R, Heathcote EJ. Sclerosing cholangitis: a focus on secondary causes. *Hepatology* 2006; **44**: 1063–74. doi: <https://doi.org/10.1002/hep.21405>
  56. Mourad MM, Algarni A, Lioussis C, Bramhall SR. Aetiology and risk factors of ischaemic cholangiopathy after liver transplantation.

- World J Gastroenterol* 2014; **20**: 6159–69. doi: <https://doi.org/10.3748/wjg.v20.i20.6159>
57. Sandrasegaran K, Alazmi WM, Tann M, Fogel EL, McHenry L, Lehman GA. Chemotherapy-Induced sclerosing cholangitis. *Clin Radiol* 2006; **61**: 670–8. doi: <https://doi.org/10.1016/j.crad.2006.02.013>
  58. Martins P, Verdelho Machado M. Secondary sclerosing cholangitis in critically ill patients: an underdiagnosed entity. *GE Port J Gastroenterol* 2020; **27**: 103–14. doi: <https://doi.org/10.1159/000501405>
  59. Roth NC, Kim A, Vitkovski T, Xia J, Ramirez G, Bernstein D, et al. Post-COVID-19 cholangiopathy: a novel entity. *Am J Gastroenterol* 2021; **116**: 1077–82. doi: <https://doi.org/10.14309/ajg.000000000001154>
  60. Portincasa P, Krawczyk M, Machill A, Lammert F, Di Ciaula A. Hepatic consequences of COVID-19 infection. Lapping or biting? *Eur J Intern Med* 2020; **77**: 18–24. doi: <https://doi.org/10.1016/j.ejim.2020.05.035>
  61. Gossard AA, Angulo P, Lindor KD. Secondary sclerosing cholangitis: a comparison to primary sclerosing cholangitis. *Am J Gastroenterol* 2005; **100**: 1330–3. doi: <https://doi.org/10.1111/j.1572-0241.2005.41526.x>
  62. Vitellas KM, Keogan MT, Freed KS, Enns RA, Spritzer CE, Baillie JM, et al. Radiologic manifestations of sclerosing cholangitis with emphasis on Mr cholangiopancreatography. *Radiographics* 2000; **20**: 959–75. doi: <https://doi.org/10.1148/radiographics.20.4.g00j04959>
  63. Lazaridis KN, LaRusso NF. Primary sclerosing cholangitis. *N Engl J Med Overseas Ed* 2016; **375**: 1161–70. doi: <https://doi.org/10.1056/NEJMra1506330>
  64. Mago S, Wu GY. Primary sclerosing cholangitis and primary biliary cirrhosis overlap syndrome: a review. *J Clin Transl Hepatol* 2020; **8**: 1–11. doi: <https://doi.org/10.14218/JCTH.2020.00036>
  65. Carrasco-Avino G, Schiano TD, Ward SC, Thung SN, Fiel MI. Primary sclerosing cholangitis: detailed histologic assessment and integration using bioinformatics highlights arterial fibrointimal hyperplasia as a novel feature. *Am J Clin Pathol* 2015; **143**: 505–13. doi: <https://doi.org/10.1309/AJCPVKFVIPRBXQR2>
  66. Selvaraj EA, Culver EL, Bungay H, Bailey A, Chapman RW, Pavlides M. Evolving role of magnetic resonance techniques in primary sclerosing cholangitis. *World J Gastroenterol* 2019; **25**: 644–58. doi: <https://doi.org/10.3748/wjg.v25.i6.644>
  67. Chapman RW, Williamson KD. Are dominant strictures in primary sclerosing cholangitis a risk factor for cholangiocarcinoma? *Curr Hepatol Rep* 2017; **16**: 124–9. doi: <https://doi.org/10.1007/s11901-017-0341-2>
  68. Boraschi P, Donati F. Biliary-Enteric anastomoses: spectrum of findings on Gd-EOB-DTPA-enhanced Mr cholangiography. *Abdom Imaging* 2013; **38**: 1351–9. doi: <https://doi.org/10.1007/s00261-013-0007-7>
  69. Bastati N, Beer L, Mandorfer M, Poetter-Lang S, Tamandl D, Bican Y, et al. Does the functional liver imaging score derived from gadoteric acid-enhanced MRI predict outcomes in chronic liver disease? *Radiology* 2020; **294**: 98–107. doi: <https://doi.org/10.1148/radiol.2019190734>
  70. Rupp C, Hippchen T, Bruckner T, Klötters-Plachky P, Schaible A, Koschny R, et al. Effect of scheduled endoscopic dilatation of dominant strictures on outcome in patients with primary sclerosing cholangitis. *Gut* 2019; **68**: 2170–8. doi: <https://doi.org/10.1136/gutjnl-2018-316801>
  71. Poetter-Lang S, Bastati N, Messner A, Kristic A, Herold A, Hodge JC, et al. Quantification of liver function using gadoteric acid-enhanced MRI. *Abdom Radiol* 2020; **45**: 3532–44. doi: <https://doi.org/10.1007/s00261-020-02779-x>
  72. Bastati N, Wibmer A, Tamandl D, Einspieler H, Hodge JC, Poetter-Lang S, et al. Assessment of orthotopic liver transplant graft survival on gadoteric acid-enhanced magnetic resonance imaging using qualitative and quantitative parameters. *Invest Radiol* 2016; **51**: 728–34. doi: <https://doi.org/10.1097/RLI.000000000000286>
  73. European association for the study of the liver. electronic address eee, European association for the study of the L. *EASL Clinical Practice Guidelines: The diagnosis and management of patients with primary biliary cholangitis*. *J Hepatol* 2017; **67**: 145–72.
  74. Idilman IS, Venkatesh SH, Eaton JE, Bolan CW, Osman KT, Maselli DB, et al. Magnetic resonance imaging features in 283 patients with primary biliary cholangitis. *Eur Radiol* 2020; **30**: 5139–48. doi: <https://doi.org/10.1007/s00330-020-06855-0>
  75. Meng Y, Liang Y, Liu M. The value of MRI in the diagnosis of primary biliary cirrhosis and assessment of liver fibrosis. *PLoS One* 2015; **10**: e0120110. doi: <https://doi.org/10.1371/journal.pone.0120110>
  76. Huang Y-Q. Recent advances in the diagnosis and treatment of primary biliary cholangitis. *World J Hepatol* 2016; **8**: 1419–41. doi: <https://doi.org/10.4254/wjh.v8.i33.1419>
  77. Terayama N, Makimoto KP, Kobayashi S, Nakanuma Y, Sasaki M, Saito K, et al. Pathology of the spleen in primary biliary cirrhosis: an autopsy study. *Pathol Int* 1994; **44**(10-11): 753–8. doi: <https://doi.org/10.1111/j.1440-1827.1994.tb02922.x>
  78. Murata Y, Abe M, Hiasa Y, Azemoto N, Kumagi T, Furukawa S, et al. Liver/spleen volume ratio as a predictor of prognosis in primary biliary cirrhosis. *J Gastroenterol* 2008; **43**: 632–6. doi: <https://doi.org/10.1007/s00535-008-2202-9>
  79. Schreiber I, Regev A. Recurrent primary biliary cirrhosis after liver transplantation—the disease and its management. *MedGenMed* 2006; **8**: 30.
  80. Montano-Loza AJ, Bhanji RA, Wasilenko S, Mason AL. Systematic review: recurrent autoimmune liver diseases after liver transplantation. *Aliment Pharmacol Ther* 2017; **45**: 485–500. doi: <https://doi.org/10.1111/apt.13894>
  81. Zeng N, Duan W, Chen S, Wu S, Ma H, Ou X, et al. Epidemiology and clinical course of primary biliary cholangitis in the Asia-Pacific region: a systematic review and meta-analysis. *Hepatol Int* 2019; **13**: 788–99. doi: <https://doi.org/10.1007/s12072-019-09984-x>
  82. Abraham M, Khosroshahi A. Diagnostic and treatment workup for IgG4-related disease. *Expert Rev Clin Immunol* 2017; **13**: 867–75. doi: <https://doi.org/10.1080/1744666X.2017.1354698>
  83. Löhr J-M, Beuers U, Vujasinovic M, Alvaro D, Frøkjær JB, Buttgerit F, et al. European Guideline on IgG4-related digestive disease - UEG and SGF evidence-based recommendations. *United European Gastroenterol J* 2020; **8**: 637–66. doi: <https://doi.org/10.1177/2050640620934911>
  84. Varghese JL, Fung AWS, Mattman A, Quach TTT, Gauiran DTV, Carruthers MN, et al. Clinical utility of serum IgG4 measurement. *Clin Chim Acta* 2020; **506**: 228–35. doi: <https://doi.org/10.1016/j.cca.2020.04.001>
  85. Lanzillotta M, Mancuso G, Della-Torre E. Advances in the diagnosis and management of IgG4 related disease. *BMJ* 2020; **369**: m1067. doi: <https://doi.org/10.1136/bmj.m1067>
  86. Hegade VS, Sheridan MB, Huggett MT. Diagnosis and management of IgG4-related disease. *Frontline Gastroenterol* 2019; **10**: 275–83. doi: <https://doi.org/10.1136/flgastro-2018-101001>
  87. Takagi Y, Kubota K, Takayanagi T, Kurita Y, Ishii K, Hasegawa S, et al. Clinical features of isolated proximal-type immunoglobulin G4-related sclerosing cholangitis. *Dig Endosc* 2019; **31**: 422–30. doi: <https://doi.org/10.1111/den.13320>

88. Björnsson E, Chari ST, Smyrk TC, Lindor K. Immunoglobulin G4 associated cholangitis: description of an emerging clinical entity based on review of the literature. *Hepatology* 2007; **45**: 1547–54. doi: <https://doi.org/10.1002/hep.21685>
89. Kamisawa T, Okazaki K. Diagnosis and treatment of IgG4-related disease. *Curr Top Microbiol Immunol* 2017; **401**: 19–33. doi: [https://doi.org/10.1007/82\\_2016\\_36](https://doi.org/10.1007/82_2016_36)
90. Leise MD, Poterucha JJ, Talwalkar JA. Drug-Induced liver injury. *Mayo Clin Proc* 2014; **89**: 95–106. doi: <https://doi.org/10.1016/j.mayocp.2013.09.016>
91. Visentin M, Lenggenhager D, Gai Z, Kullak-Ublick GA. Drug-Induced bile duct injury. *Biochim Biophys Acta Mol Basis Dis* 2018; **1864**(4 Pt B): 1498–506. doi: <https://doi.org/10.1016/j.bbadis.2017.08.033>
92. European association for the study of the liver. electronic address eee, clinical practice guideline panel C, panel M, representative EGB. *EASL Clinical Practice Guidelines: Drug-induced liver injury. J Hepatol* 2019; **70**: 1222–61.
93. Alessandrino F, Tirumani SH, Krajewski KM, Shinagare AB, Jagannathan JP, Ramaiya NH, et al. Imaging of hepatic toxicity of systemic therapy in a tertiary cancer centre: chemotherapy, haematopoietic stem cell transplantation, molecular targeted therapies, and immune checkpoint inhibitors. *Clin Radiol* 2017; **72**: 521–33. doi: <https://doi.org/10.1016/j.crad.2017.04.003>
94. Shea WJ, Demas BE, Goldberg HI, Hohn DC, Ferrell LD, Kerlan RK. Sclerosing cholangitis associated with hepatic arterial FUDR chemotherapy: radiographic-histologic correlation. *AJR Am J Roentgenol* 1986; **146**: 717–21. doi: <https://doi.org/10.2214/ajr.146.4.717>
95. Capra F, Nicolini N, Morana G, Guglielmi A, Capelli P, Vantini I. Vanishing bile duct syndrome and inflammatory pseudotumor associated with a case of anabolic steroid abuse. *Dig Dis Sci* 2005; **50**: 1535–7. doi: <https://doi.org/10.1007/s10620-005-2876-2>
96. Saunders MD, Shulman HM, Murakami CS, Chauncey TR, Bensinger WI, McDonald GB. Bile duct apoptosis and cholestasis resembling acute graft-versus-host disease after autologous hematopoietic cell transplantation. *Am J Surg Pathol* 2000; **24**: 1004–8. doi: <https://doi.org/10.1097/0000478-200007000-00012>